SECTION 86

THE CONSTRAINT OF SUN GLINT ON VISIBLE DATA GATHERED BY EARTH SATELLITES

by

Alan E. Strong
National Oceanic and Atmospheric Administration
Washington, D. C. 20031

INTRODUCTION

Viewing Earth's oceans from increasing altitudes results in an expanding sunglint area on the ocean scene. At the equinox an aircraft flying along the equator at 10,000 feet experiences little difficulty viewing a dark ocean from nadir at 1500 local time. From the geosynchronous altitude of ATS (19,300 miles) a similar view of the ocean suffers from sunglint "contamination" at nadir for several hours either side of local noon. Oceanographers hoping to employ environmental satellites at intermediate altitudes for ocean color studies must be aware of and operate with this sunglint constraint when viewing these low radiance levels. This paper presents sunglint simulation from selected satellite orbits in an attempt to optimize the selection of an orbit suitable for ocean color measurements.

SPACE VIEWED OCEAN SUNGLINT

It is important to remember that as the Earth is viewed from increasing altitude the solid angle subtended by Earth decreases. Naturally, the solid angle subtended by the sun remains virtually constant. Such geometric conditions cause the glitter pattern from an ocean to expand in areal extent as the observational altitude increases. This is easily illustrated by comparing the photographs in Figs. 1 and 2. Fig. 1 shows the sunglint pattern over the mid-equatorial Pacific viewed from ESSA 9 altitude (780 n. miles). The ATS-I photograph in Fig. 2 is from the geosynchronous altitude of 19,300 nautical miles. From similar photographs it can be easily demonstrated that although a view of the ocean at nadir at 1400 local time would not be contaminated by glitter, viewing from 780 n. miles would find the glitter area had expanded sufficiently to contaminate nadir.

SUNGLINT SIMULATION FOR AN EARTH ORBITING RADIOMETER

During the preliminary planning phases of satellite oceanographic missions it became obvious that the sun would be a driving function for ocean color measurements. Some recent ocean color work by Duntley (1971) has indicated that a minimum solar zenith angle of 35° is necessary. He stated that the maximum solar zenith is dictated by the various angles involved in contamination of high solar zeniths with sunglint.

We have taken the same model that was developed to simulate the sunglint patterns (Strong and Ruff, 1970) coming from a range of ocean roughnesses and observed by the "old" ESSA vidicon photographs (similar to Fig. 1) and reoriented the model to illustrate the reflection pattern as would be seen by a scanning radiometer (SR). The Improved TIROS Operational Satellite (ITOS) is converting from the vidicon to the SR during 1972. Figure 3 provides an example of visible imagery from the NOAA-1 satellite SR. The curves overlaying the imagery show solar zenith angles at Earth's surface. Since the NOAA satellites are currently ascending across the equator at 1530 local time the higher solar zeniths occur to the west of the subsatellite track (nadir) - north-south lies approximately through the middle of the image. Greenland is apparent at the top of the image. The major water body on this example is the Mediterranean Sea. In the sunglint region over the Mediterranean Sea a narrow band of glitter can be seen to extend from Malta, around the western tip of Sicily, and then northward between Sardinia and Italy. The AVCS picture from ESSA 9 and shown in Fig. 4 was taken within a few minutes of the SR data and illustrates not only the marked difference between the performance of the two sensors but also that the sunglint region off Sicily is indeed free of clouds. Similar anomalous glitter features have been discussed previously (McClain and Strong, 1969) and unveil areas that are devoid of small-scale surface roughness. The concurrent surface weather charts for the Mediterranean area indicate these calm areas most likely mark the center of sea breeze circulations off the coasts - mesoscale high pressure regions.

Employing surface wave slope statistics from Cox and Munk (1956) glitter patterns have been similated for 5 m $\sec^{-1}$ and 10 m $\sec^{-1}$ surface wind speeds. These patterns, shown in Figs. 5 and 6, were simulated to correspond to the NOAA-1 orbit and imagery shown in Fig. 3. Units represent percent reflectance at the surface and consider no corrections for atmospheric or surface water layer attenuation or scattering. The 0.1% isophote has been included as some oceanographers feel this is the sensitivity to which ocean color sensors need to be sensitive (Clark, et at., 1970).

From the last two figures it is obvious that 1530 local time is not a desirable time to measure ocean color from space as the maximum glint occurs under solar zeniths between 30 and 35 degrees. It is apparent that a near-noon orbit provides the only way to obtain a high solar zenith. Glitter simulation was made for the same altitude (780 n. mi.) but revised to consider an equatorial ascention of local noon. Figure 7 shows the resulting solar zenith curves over the imagery for 25 June. It is interesting to compare the resulting glitter patterns in Figs. 8 and 9 as with those patterns from the afternoon orbit. Wind speeds of 5 m sec^{-1} and 10 m sec^{-1}, respectively, were again simulated. Since the glint falls nearly beneath the satellite more reflected energy reaches the satellite sensor. However, large areas either side of the glitter have a high solar zenith that should permit ocean color measurements outside the glitter pattern that was simply not possible from the afternoon orbit. The 0.1% isophote for the 5 m sec^{-1} simulation never exceeds a 15° satellite viewing angle from nadir.

CONCLUSIONS

It appears from the ocean sunglint simulations presented that ocean color sensing from satellite may be most productive during a near-noon polar orbit. Sunglint along the subsatellite track will contaminate much of the ocean view out to 10 to 15 degrees either side of nadir but useful data either side of the nadir-oriented glint will be possible under the necessary high solar illumination. If fact, some limited oceanic observations may be possible under 5 and 10 degree solar zenith angles.

With a good dynamic range sensor, surface roughness measurements could be made throughout the glitter region. Two advantages are available for noon-viewed glitter (1) reflectance is maximized, and (2) the central location migrates least with changing wind speed (this effect can be seen by comparing Figs. 5 and 6 with 8 and 9). These two features make point reflectance measurements more strongly wind dependent and reduce the wind speed uncertainty when compared with satellite measurements before or after local noon.

REFERENCES

1. Duntley, S. W., August 1971 briefing to NASA's Earth Observatory Satellite Mission Review Group at Goddard Space Flight Center.

2. Strong, A. E. and I. S. Ruff, 1970. Utilizing satellite-observed solar reflections from the sea surface as an indicator of surface wind speed, Remote Sensing of Environment, 1: 181-185.

3. McClain, E. P. and A. E. Strong, 1969: On cluomalous dark patches is satellite-viewed sunglint areas, Monthly Weather Review, 97(12): 875-884.

4. Cox, C. and W. Munk, 1956: Slopes of the sea surface deduced from photographs of sun glitter, Bulletin Scripps Institute of Oceanography, 6(9): 401-488.

5. Clark, G. L., Ewing, G. C. and C. J. Lorenzen, 1970: Spectra of backscattered light fromthe sea obtained from aircraft as a measure of chlorophyll concentration, Science, 167 (3921).

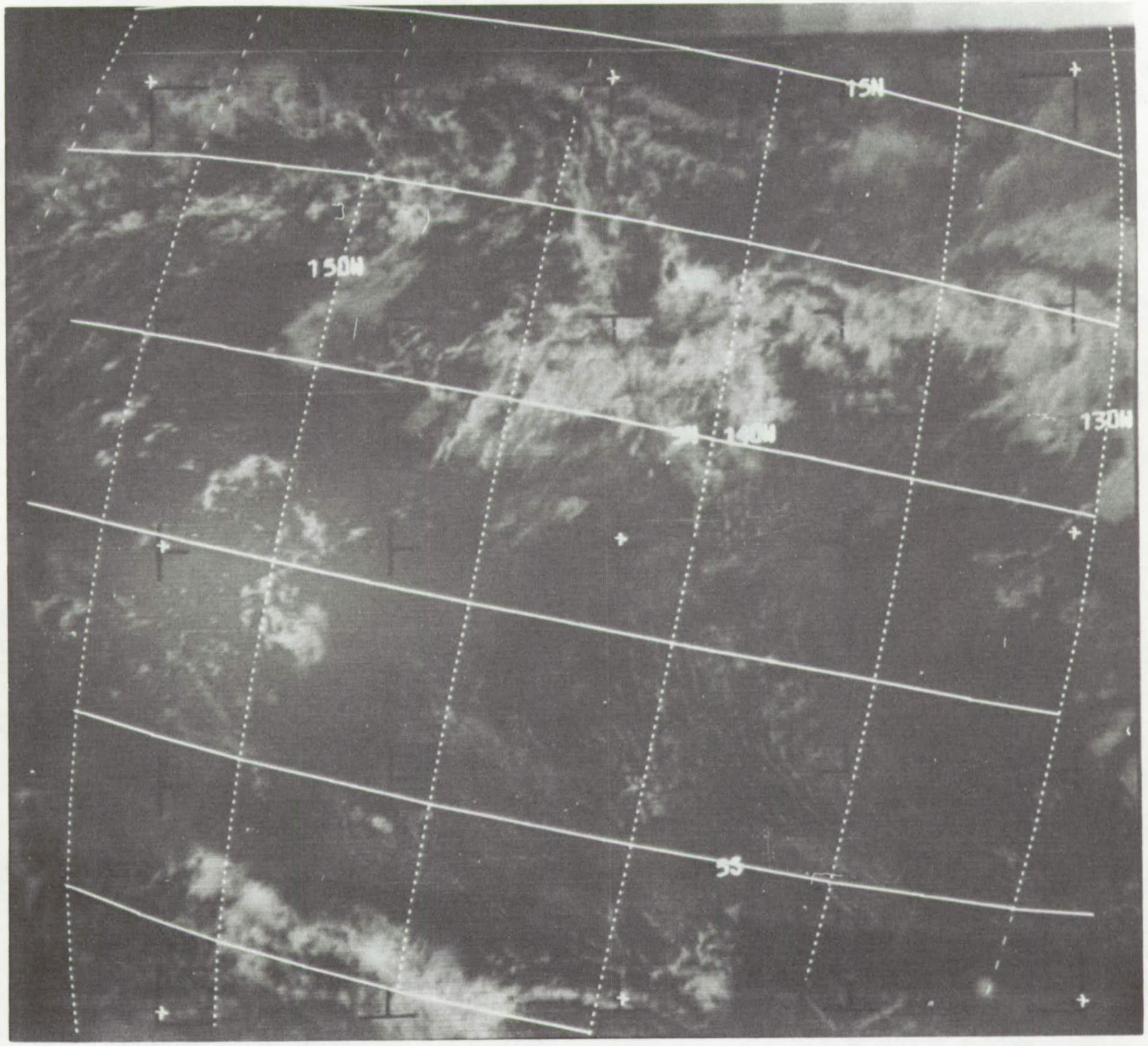

Fig. 1. ESSA 9 AVCS Photograph, 28 October 1971. Compare sunglint coverage of ocean scene in Fig. 1 with Fig. 2.

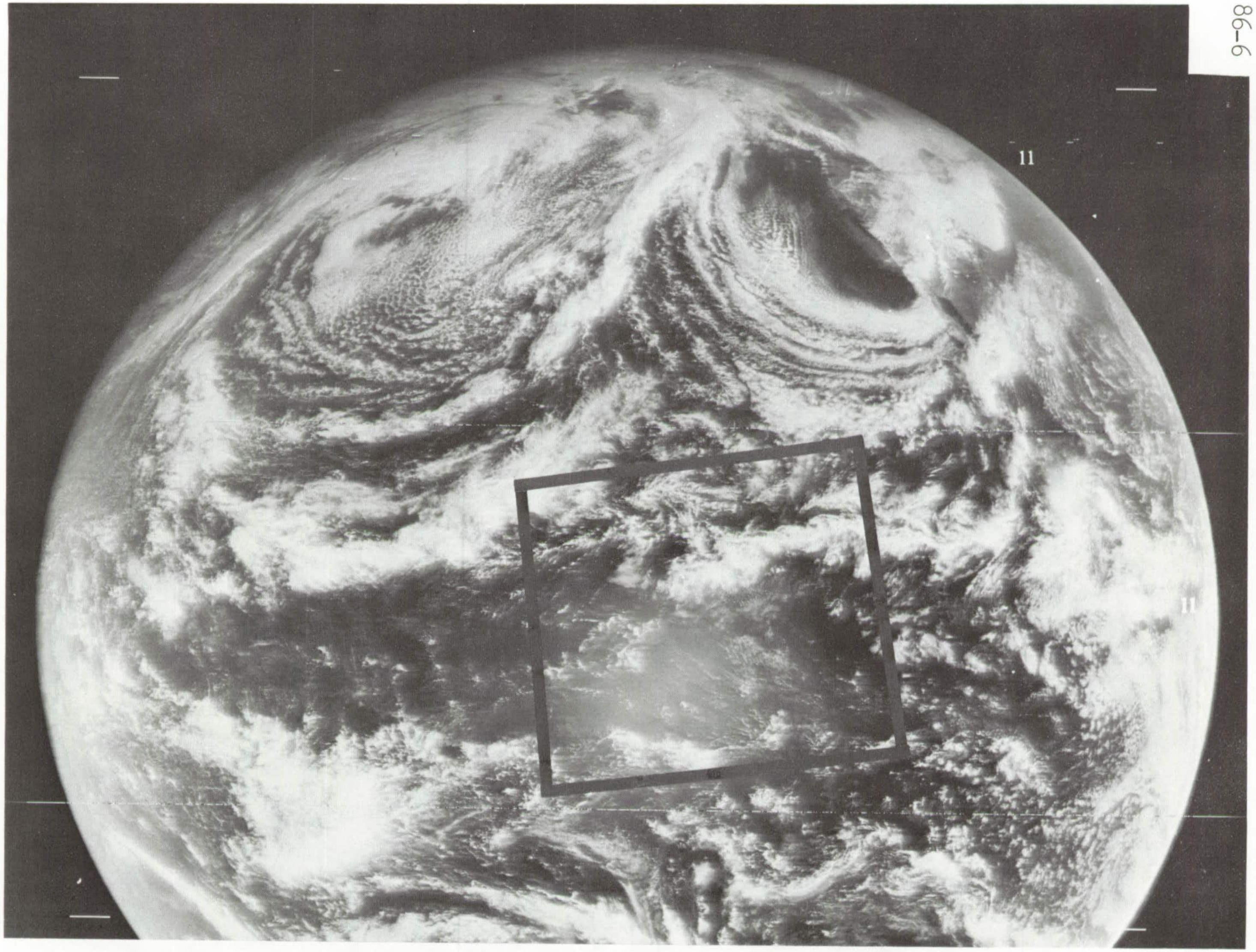

Fig. 2. ATS 1, 28 October 1971. Compare sunglint coverage of ocean scene in Fig. 2 with Fig. 1. Box shows approximate area covered by Fig. 1.

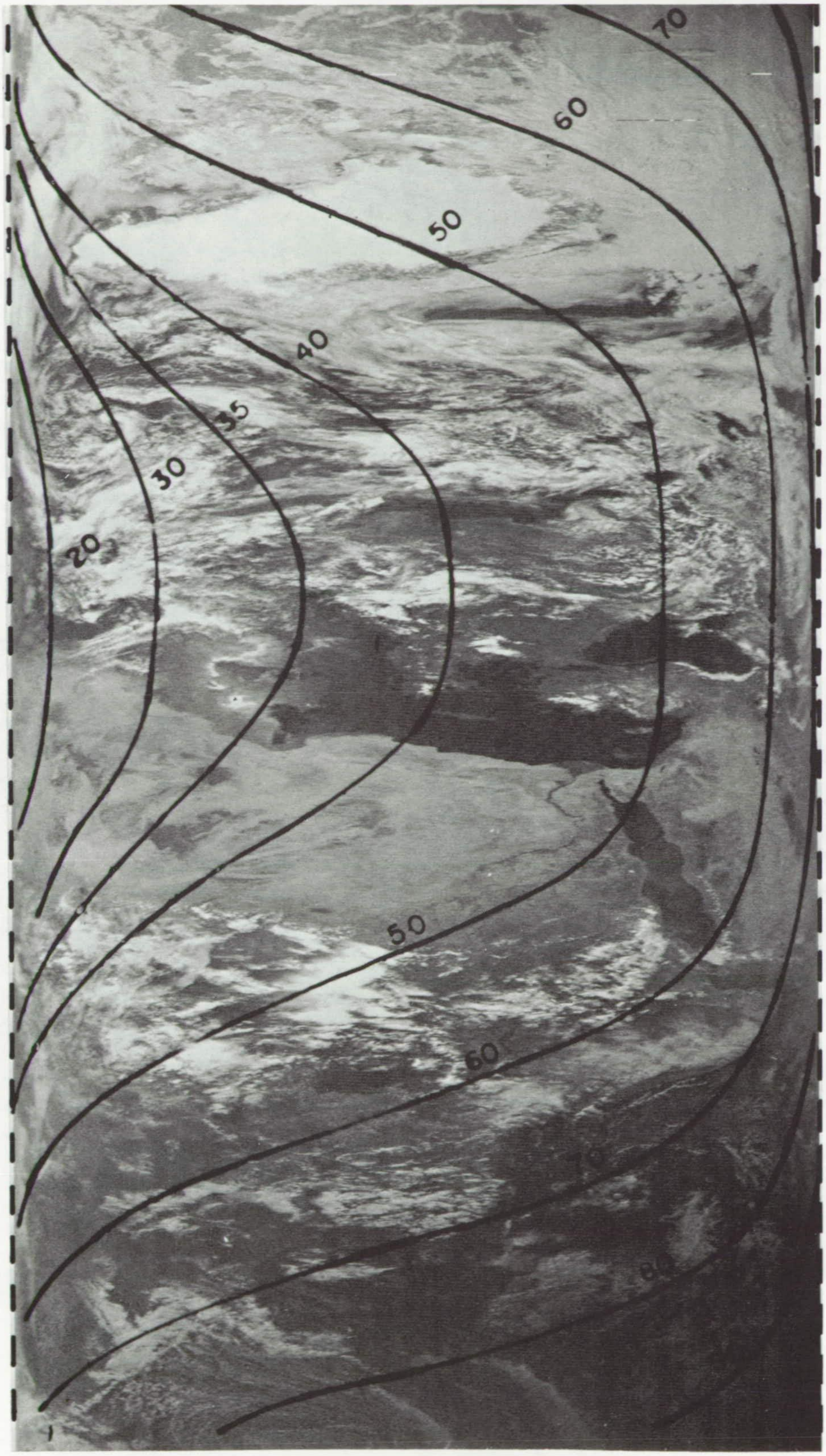

Fig. 3. NOAA-1 Scanning Radiometer Visible Imagery, 25 June 1971. Note sunglint in Mediterranean Sea. Solar zenith angles are Earth-located for 1530 local time, 780 nautical mile orbit.

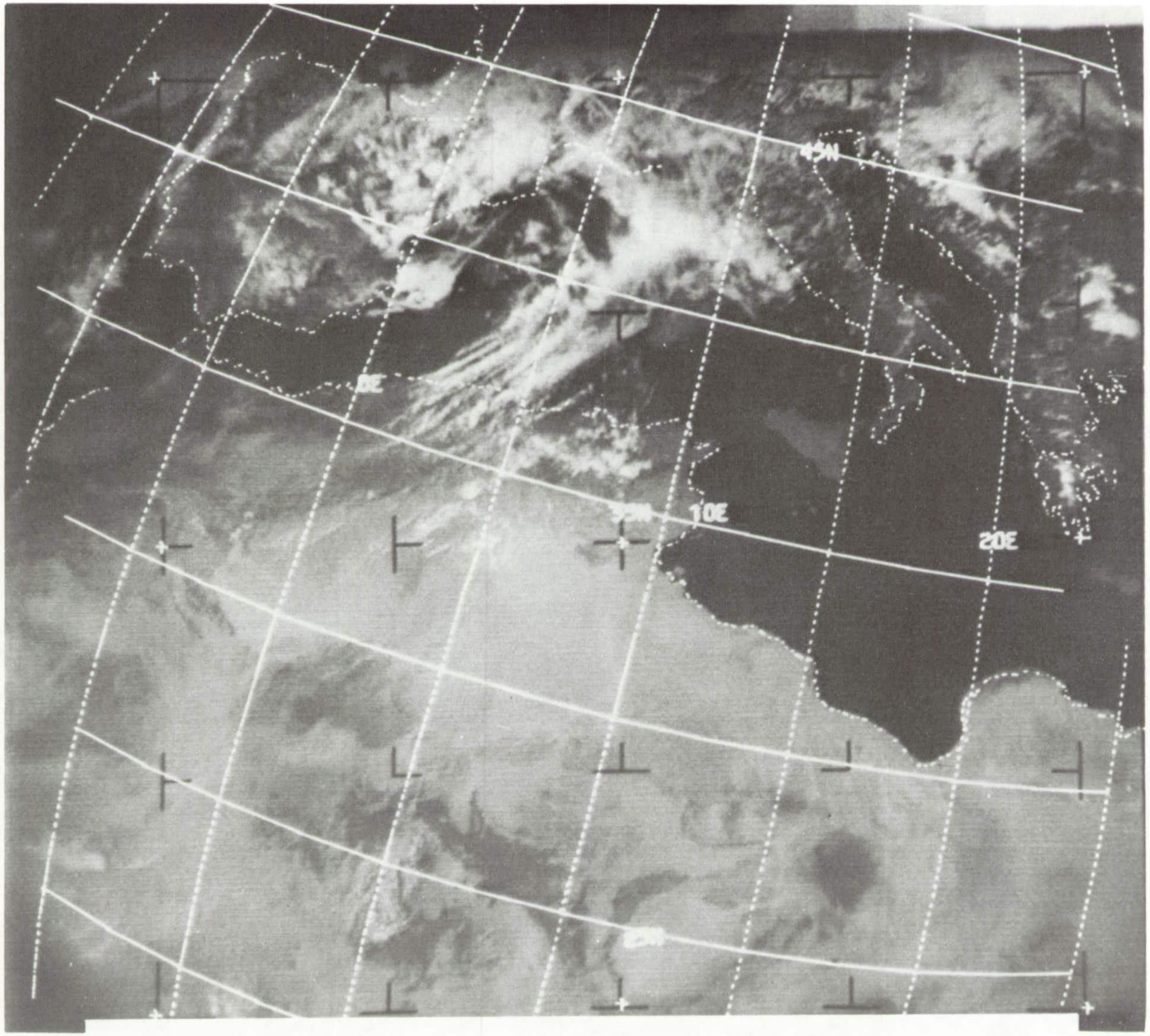

Fig. 4. ESSA 9 AVCS Photograph. 25 June 1971. Taken approximately same time as imagery over Mediterranean shown in Fig. 3. Note clear sky mode over Sicily.

Fig. 5. NOAA-1. Visible Imagery with reflectance ratio for surface under 5 m sec-1 wind.

Fig. 6. Same as Fig. 5 but for 10 m sec^{-1} wind.

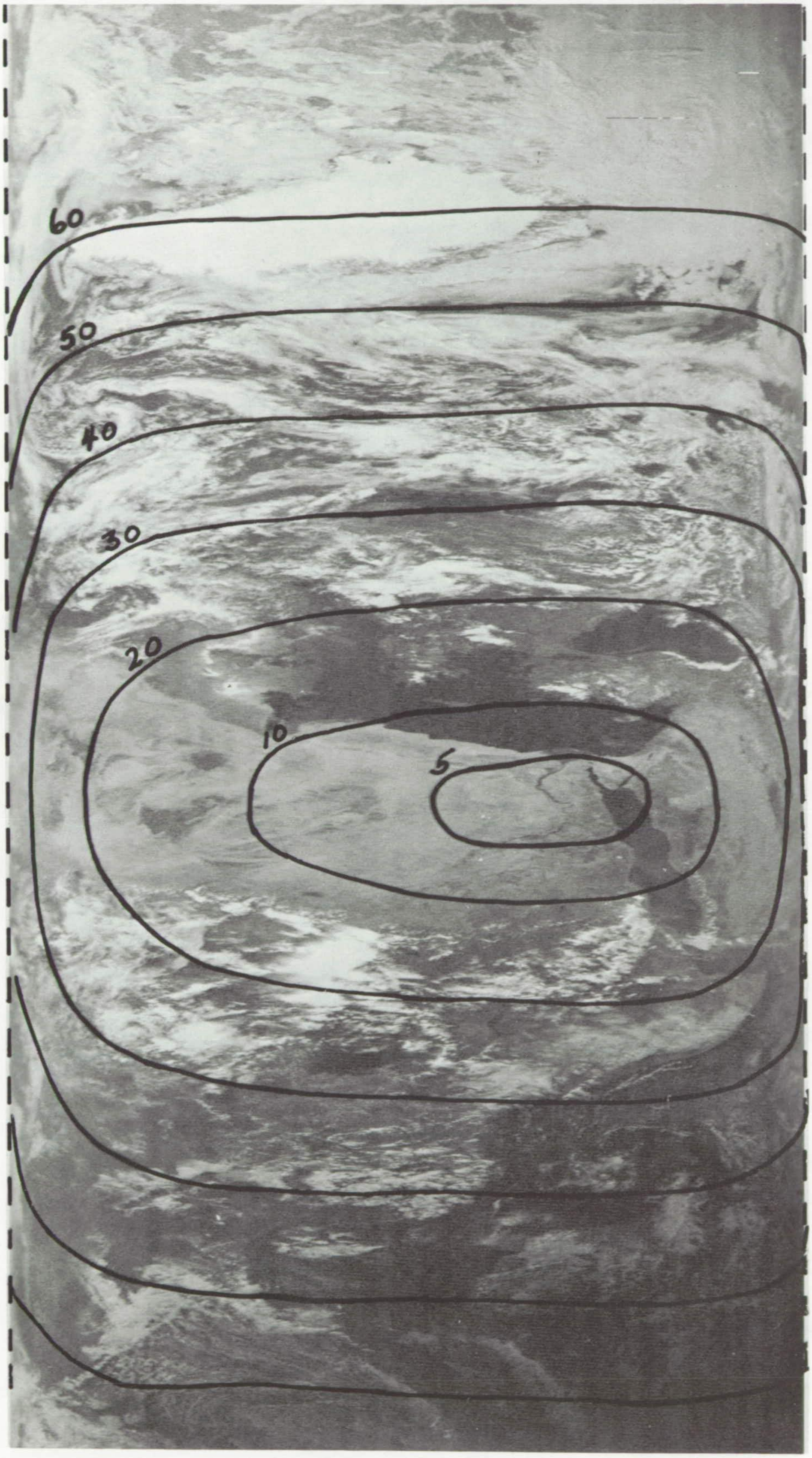

Fig. 7. NOAA-1 imagery with simulated solar zeniths for noon orbit at 780 n. miles.

Fig. 8. Reflectance ratios for Fig. 7 simulation with surface wind of 5 m sec^{-1}.

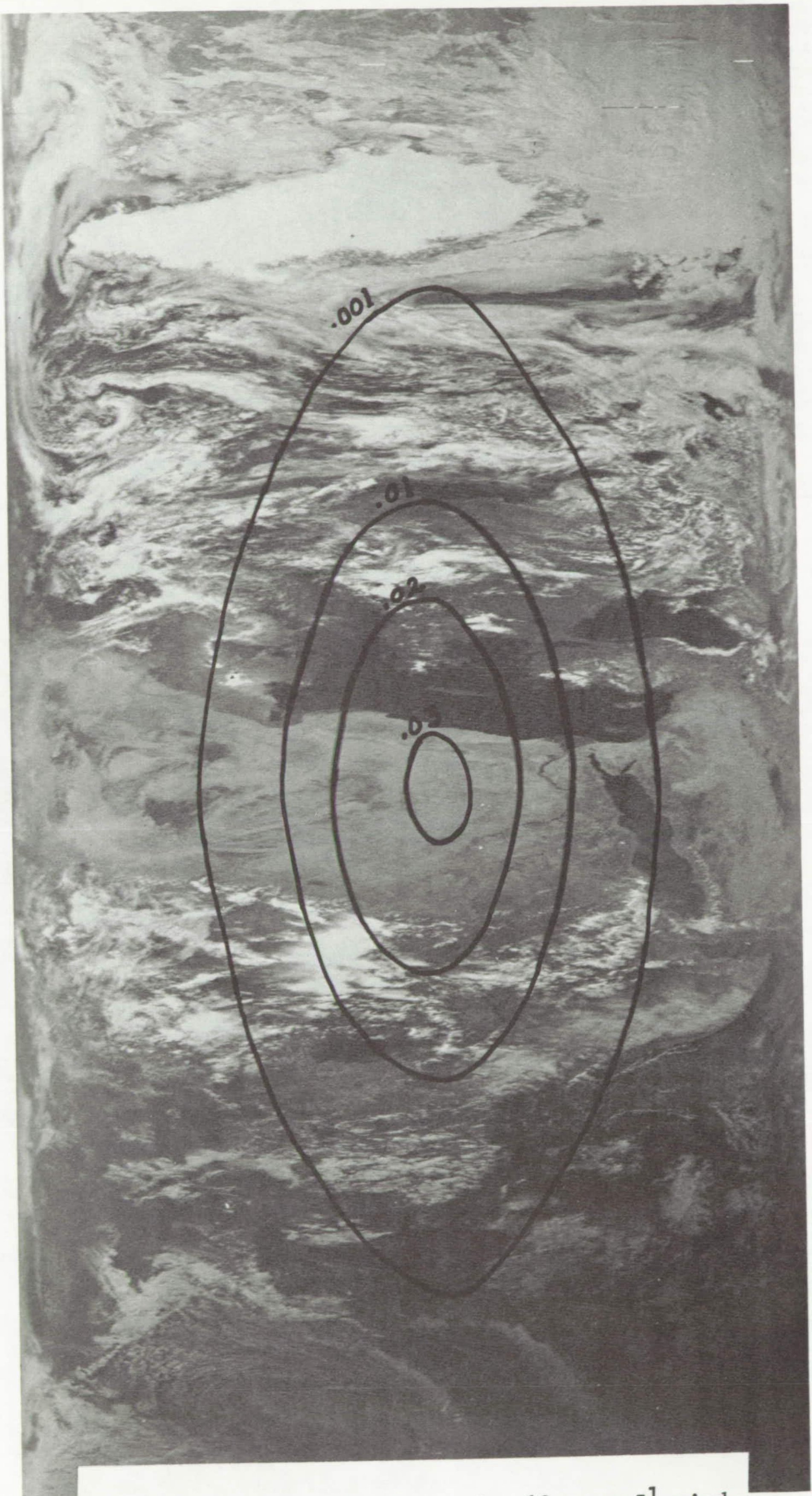

Fig. 9. Same as Fig. 8 but for 10 m sec^{-1} wind.